

## Research Paper

**Cite this article:** Chakraborty A, Ram G, Mandal D (2022). Time-modulated linear array synthesis with optimal time schemes for the simultaneous suppression of sidelobe and sidebands. *International Journal of Microwave and Wireless Technologies* **14**, 768–780. <https://doi.org/10.1017/S175907872100088X>

Received: 25 December 2020  
Revised: 16 May 2021  
Accepted: 18 May 2021  
First published online: 11 June 2021

### Key words:

Time-modulated array; sideband radiations; sidelobe level; particle swarm optimization; wavelet mutation; harmonics

### Author for correspondence:

Avishek Chakraborty,  
E-mail: [avishekdreamz@gmail.com](mailto:avishekdreamz@gmail.com)

# Time-modulated linear array synthesis with optimal time schemes for the simultaneous suppression of sidelobe and sidebands

Avishek Chakraborty<sup>1</sup> , Gopi Ram<sup>2</sup>  and Durbadal Mandal<sup>1</sup> 

<sup>1</sup>Department of Electronics and Communication Engineering, National Institute of Technology, Durgapur, West Bengal 713209, India and <sup>2</sup>Department of Electronics and Communication Engineering, National Institute of Technology, Warangal, Telangana 506004, India

## Abstract

An efficient analysis of time-modulated array (TMA) toward realizing less-attenuating radiation patterns with simultaneously suppressed sidelobe and sidebands is presented in this paper. In this framework, an optimal outer element-controlled time sequence is derived. The proposed time scheme, along with optimized array excitations, is profitably applied for the desired solution. TMAs are considered unconventional alternatives to the phased arrays. The desired array radiation features can be attained by periodically enabling and disabling the array elements through high-speed switches. Despite the advantages of architectural simplicity and real-time reconfigurability of periodic time sequences, time-domain antenna arrays inherently generate unavoidable sideband radiations (SRs). The undesired SRs obtained at multiple harmonics around the carrier frequency of the array resembles power loss in unintended directions. This paper aims to minimize the SRs as well as the sidelobe level (SLL) for an efficient analysis of time-modulated linear array (TMLA) with high-directive radiation patterns. The starting instants and the period of on-times are optimized to generate a unique shifted time scheme for the edge elements of the TMLA to reduce the sideband levels (SBLs). The array excitations and the uniform spacing between the elements are also optimized together with the shifted time scheme for the coveted solution. Other methods of suppressing SLLs and SBLs with shifted pulse schemes and sub-sectioned pulse schemes are also presented for a fair comparison. Modified versions of the particle swarm optimization algorithm (PSO) are applied for the desired solutions. The optimal results attained by wavelet mutation-based novel PSO is compared with the conventional PSO and the modified novel PSO-based results. The representative results are reported, and the superior performance abilities of the proposed method compared to other published studies are assessed.

## Introduction

The introduction of “time” as an additional parameter to control antenna array radiation patterns was originated with the pioneering work of Shanks and Bickmore [1]. “Time” is often considered as the fourth dimension, which can be accurately controlled by inserting rapid switches in the array feeding network [2]. Time-modulated arrays (TMAs) have evolved as unconventional alternatives to phased arrays due to their reconfiguration capabilities [3]. The simple periodic on–off sequence also increases the architectural simplicity by eliminating the phase shifters for a profitable solution [4]. The adaptabilities of time-domain arrays have further been explored with electronic scanning [5] and also validated experimentally for nearly ultra-low sidelobe levels (SLLs) [6]. The interest in TMAs has been accelerated with emerging optimization algorithms as a means to control the beam pattern through optimized pulse driving sequences [7, 8]. The reliability of periodic time sequence to obtain the desired radiation characteristics has also come with the inherent generation of sideband radiations (SRs) at multiples of modulated frequencies usually considered as power loss in undesired directions [9]. Several studies have been carried out with optimized time sequences to reduce SRs [10, 11]. The sideband levels (SBLs) have been minimized with optimized shifted pulses [12], sub-sectioned time steps [13, 14], and nonuniformly excited thinned arrays [15]. The joint optimization approach using convex programming and evolutionary techniques are also studied for the synthesis of large-scale heterogeneous TMAs [16, 17]. Research on TMAs has further been extended by proposing iterative convex optimization algorithms for efficient pencil beam synthesis [18]. Some hybridized approaches to generate pencil beam patterns as well as shaped beam patterns have been investigated by constraining dynamic range ratios (DRRs) of TMAs [19]. An optimal pulse shifting approach has also been introduced to minimize the SLL and SBL of linear TMAs at the same time [20]. The optimization of shifted on-off time sequences required to generate the desired radiation patterns, decreases the efficiency of TMA as the off-states account for energy absorption. Several methods for the simultaneous reduction of SLLs

and SBLs have also been discussed with different switching configurations to enhance the gain [21], directivity [22], and the overall efficiency [23] of the array. Pulse-shaped strategies [24] and other unified time and frequency domain studies have been performed to explore different switching schemes [25]. The accurately modeled circuit-level analysis of TMAs considering the dynamic behavior of nonlinear switching elements has also been investigated [26, 27]. A different perspective by exploiting the undesired SRs has unfolded the use of TMAs for the direction of arrival estimation [28]. The multiple independent harmonic patterns generated at different frequencies have also been enhanced for secure communication [29, 30]. The potentialities of TMAs for beamforming [31, 32] and beam steering [33, 34] applications have been addressed with appropriate time sequences. TMAs for monopulse sum-difference patterns [35] and multi-harmonic steered patterns [36, 37] have been discussed with controlled radiation properties. Multiple optimized patterns of TMAs [38] have also been generated for cognitive radios [39, 40] and multiple-input multiple-output systems [41, 42], which further enhances the diversity and multifunctional capabilities.

Most of the already reported literature related to SLL and SBL reduction in TMAs have considered either conventional or analytical techniques to achieve a desired solution. The time sequences are optimized in [10] to suppress the SLL and SBLs as low as possible. An optimized pulse-shifted time scheme has been derived in [12] by considering total ON-times of each element equal to a  $-30$  dB Chebyshev distribution. The sub-sectional optimized time scheme has also been proposed for SLL and SBL reduction [13]. A different approach of deriving the shifted time scheme has been proposed in [21] by setting the target SLL to  $-30$  dB. The optimal time scheme for the desired radiation pattern generation with a target SLL and SBL of  $-30$  and  $-25$  dB, respectively has also been discussed in [23]. Two different examples have been proposed in [29], where a certain number of elements are kept in switched-on condition and the on-times for the rest of the elements are optimized. The first example has proposed a time scheme with at least two elements switched-on for every instant of the modulation period, whereas, in the second example at least 10 elements are kept in switched-on condition for every instant of the total modulation period [29]. The target SLLs for both the methods have been selected as  $-20$  dB, and then tried to minimize the SBLs as low as possible [29]. Because of the conflicting nature of SLLs and SBLs, either lowered SLLs or lowered SBLs have been obtained with these methods, so far. A balance between these two has also been achieved in some cases by lowering the SLLs and SBLs simultaneously to some extent. The scope of minimizing the SLL and SBLs simultaneously is still a serious research concern for TMAs. These challenging issues are addressed in this paper by proposing a unique method where ultra-low SLL ( $<-40$  dB) and a simultaneous reduction in SBLs as low as possible is targeted. The method proposed here is completely different from the already reported literature and unique in the sense that a joint optimization of excitations and time sequences of only the four outer elements are performed, whereas in all the reported literature, only the time sequences were considered.

The aim of this paper is to minimize the SLL and SBLs of the time-modulated linear array (TMLA) while improving the directivity and the overall efficiency of the array at the same time. Toward this purpose, the time sequences of outer elements of the array are optimized along with the spacing between elements

and the array excitations for the desired solution. To achieve the proposed time scheme, the on-time durations and the starting instants of the edge elements of the TMLA are taken into account for optimization within the specified modulation period. The remaining elements are switched on for the entire time period, which also reduces the computational burden. The off-states in a time scheme bear a resemblance to the energy consumed in the array feeding network due to the absorptive nature of high-speed switches. The proposed time scheme also gets the better of this problem to a great extent and increases the power handling capability as well as the efficiency of the array. Other methods of suppressing the SLL and SBLs by optimally shifted time schemes and sub-sectioned time schemes with uniform excitations are also demonstrated for a fair comparison. The optimization process is carried out with modified versions of the particle swarm optimization (PSO). In this framework, a wavelet mutation-based novel PSO (NPSOWM) strategy is employed to get the optimal results. The conventional PSO and a modified novel PSO (NPSO) based results are also presented and compared with NPSOWM-based results. Sixteen-element TMLAs with isotropic radiating elements are used throughout this discussion, and the representative results obtained from exhaustive numerical analysis are assessed with state-of-the-art literature results.

This paper is organized with the discussion of theoretical and mathematical insights of TMLA in section "Theory and mathematical insights." The generalized time schemes associated with TMLA are also described in this section. The objectives of simultaneously suppressed SLL and SBLs and the improvements in directivity and efficiency are identified as the problem statement, and the proposed method to address these is presented in section "Problem formulation." The advantages and limitations of the proposed method compared to other SLL and SBL reduction methods are also discussed. The results obtained from the exhaustive numerical analysis are reported and assessed with other published works in section "Numerical assessment" before concluding the paper in section "Conclusion."

## Theory and mathematical insights

The generalized architecture of an  $N$ -element TMLA equipped with attenuators and high-speed switching devices for controlling the array excitations and time sequences is shown in Fig. 1. The isotropic radiating elements are aligned toward the positive  $z$ -axis with uniform spacing  $d$ . The time-averaged response of the TMLA in the far-field can be expressed as [4]:

$$AF(\theta, t) = e^{j(2\pi f_0)t} \sum_{n=1}^N I_n U_n(t) e^{j\beta(n-1)d \cos \theta} \quad (1)$$

where the array excitations are denoted with  $I_n$  ( $n = 1, 2, \dots, N$ ),  $\beta = 2\pi/\lambda_0$  is the wavenumber with  $\lambda_0$  being the wavelength at the operating frequency  $f_0$ , signals are impinging at a direction  $\theta$  from the array main axis, and the time modulating function to control the switches connected with each array element is described as  $U_n(t)$ . Due to the periodic nature of time sequences within the modulation period  $T_p$ , the time modulating function  $U_n(t)$  can be expanded into Fourier series as:

$$U_n(t) = \sum_{m=-\infty}^{\infty} a_{mn} e^{jm(2\pi f_p)t} \quad (2)$$

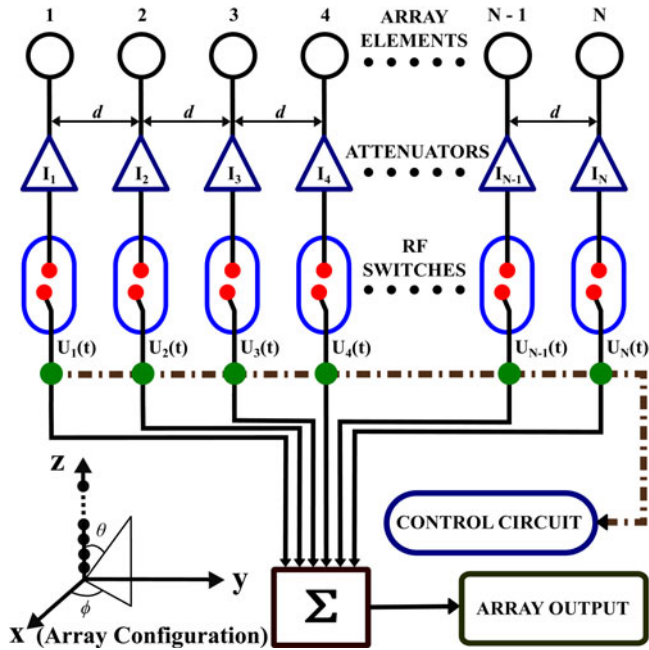


Fig. 1. Standard N-element TMLA architecture with high-speed RF switches and attenuators.

where  $f_p$  is the modulation frequency ( $f_p \ll f_0$ ), and the complex Fourier coefficient  $a_{mn}$  for the  $n^{\text{th}}$  element at  $m^{\text{th}}$  frequency ( $m = 0, \pm 1, \pm 2, \dots, \pm \infty$ ) is described as [4]:

$$a_{mn} = \frac{1}{T_p} \int_0^{T_p} U_n(t) e^{-jm(2\pi f_p)t} dt \tag{3}$$

The time-averaged array factor response can now be expanded as [4]:

$$AF(\theta, t) = \sum_{m=-\infty}^{\infty} \sum_{n=1}^N I_n a_{mn} \{e^{j\beta(n-1)d \cos \theta}\} e^{j2\pi(f_0 + mf_p)t} \tag{4}$$

The time-domain array factor response for  $m^{\text{th}}$  frequency component can further be simplified as:

$$AF_m(\theta, t) = e^{j2\pi(f_0 + mf_p)t} \sum_{n=1}^N I_n a_{mn} e^{j\beta(n-1)d \cos \theta} \tag{5}$$

The array factor for the fundamental pattern at operating frequency  $f_0$  can be obtained with  $m = 0$ , whereas the inherently generated harmonic patterns due to time-modulation can be expressed with  $m = \pm 1, \pm 2, \dots, \pm \infty$ . These harmonic radiations are usually considered as loss of power in undesired directions, which can be controlled with appropriately designed switching sequences.

The radiated power used by the fundamental pattern ( $P_0$ ), and the power radiated ( $P_T$ ) by undesired sidebands, including the fundamental pattern, can be expressed as:

$$P_0 = \int_0^{2\pi} \int_0^{\pi} |AF_0(\theta, \phi)|^2 \sin \theta d\theta d\phi \tag{6}$$

$$P_T = \sum_{m=-\infty}^{\infty} \int_0^{2\pi} \int_0^{\pi} |AF_m(\theta, \phi)|^2 \sin \theta d\theta d\phi \tag{7}$$

The directivity of the TMLA for the desired pattern can be given as [16]:

$$D = \frac{4\pi |AF_0(\theta_0, \phi_0)|^2}{\sum_{m=-\infty}^{\infty} \int_0^{2\pi} \int_0^{\pi} |AF_m(\theta, \phi)|^2 \sin \theta d\theta d\phi} \tag{8}$$

where the fundamental pattern pointing toward  $\theta = \theta_0, \phi = \phi_0$  is denoted as  $AF_0(\theta_0, \phi_0)$ , and the undesired sideband patterns at  $m^{\text{th}}$  order frequency are presented with  $AF_m(\theta, \phi)$ .

### Switching configuration

The modulating function  $U_n(t)$  can be defined with different time sequences, shown in Fig. 2. The simple on-off time scheme for the  $n^{\text{th}}$  element is shown in Fig. 2(a), where the element is on for a period of  $\tau_n$  within the modulation period  $T_p$  ( $0 \leq \tau_n \leq T_p$ ). The rise time and fall time of the pulse are denoted as  $t_1$  ( $t_1 = 0$ ) and  $t_2$ , respectively. The modulating function for the simple on-off time scheme can be expressed as:

$$U_n(t) = \begin{cases} 1, & t_1 \leq t \leq t_2 \leq T_p \text{ where } t_1 = 0 \\ 0, & \text{otherwise} \end{cases} \tag{9}$$

The Fourier excitation coefficient of the simple on-off time sequence can be derived as [13]:

$$a_{mn} = \xi_n \{\sin c(m\pi\xi_n)\} e^{-jm\pi\xi_n} \tag{10}$$

where the normalized on-time duration of the  $n^{\text{th}}$  element is denoted as  $\xi_n$  ( $= \tau_n/T_p$ ).

A modified time scheme with shifted pulse behavior is presented in Fig. 2(b), where the starting instant or the rise time of the pulse is shifted. For this shifted time scheme, the modulating function can be presented as:

$$U_n(t) = \begin{cases} 1, & 0 < t_1 \leq t \leq t_2 \leq T_p \text{ where } t_1 \neq 0 \\ 0, & \text{otherwise} \end{cases} \tag{11}$$

The corresponding complex excitation for the pulse-shifted time sequence can be derived as [13]:

$$a_{mn} = \frac{(t_2 - t_1)}{T_p} [\sin c\{m\pi f_p(t_2 - t_1)\}] e^{-jm\pi f_p(2t_1 + \tau_n)} \tag{12}$$

which can further be simplified as:

$$a_{mn} = \xi_n \{\sin c(m\pi\xi_n)\} e^{-jm\pi(2\delta_n + \xi_n)} \tag{13}$$

where the normalized starting instant of the  $n^{\text{th}}$  element is denoted as  $\delta_n$  ( $= t_1/T_p$ ). The reduction in SRs can be achieved with modified time sequences without altering the properties of the desired fundamental pattern. The starting instants and closing instants of array elements account for the simple on-off configuration of switches associated with each element of TMLA. Different possible combinations of time schemes can be generated to address different applications of TMLA.

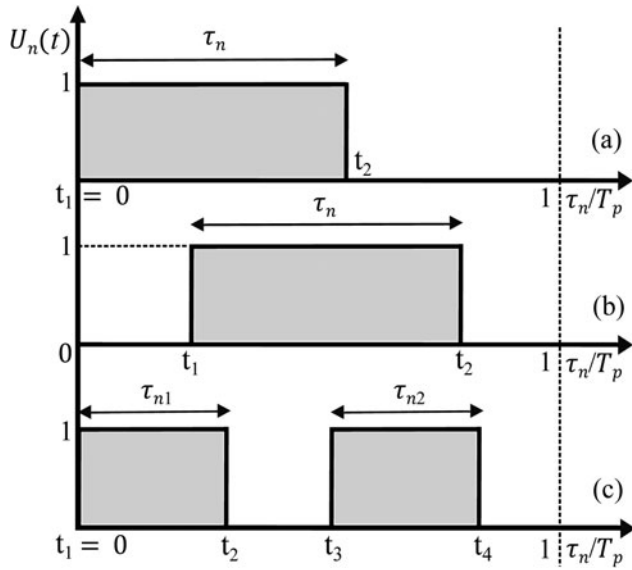


**Fig. 2.** Time sequences with (a) simple on-off pulse, (b) shifted pulse, and (c) sub-sectioned pulse.

Toward this purpose, a combined sub-sectional time sequence for the  $n^{\text{th}}$  element is also presented in Fig. 2(c), where the on-time period of each element is split up into two sub-pulses with an off-state in between. The element is switched on at  $t_1$  ( $t_1 = 0$ ) and remain in on-state up to  $t_2$  with an on-time duration of  $\tau_{n1} (= t_2 - t_1)$ . Then the element is switched off from  $t_2$  to  $t_3$  before going into an on-state again for the duration of  $\tau_{n2} (= t_4 - t_3)$ . The modulating function of sub-sectioned time scheme can be expressed as:

$$U_n(t) = \begin{cases} 1, & t_1 \leq t \leq t_2 \leq T_p \quad \text{where } t_1 = 0 \\ 1, & t_3 \leq t \leq t_4 \leq T_p \quad \text{where } t_1 < t_3 \\ 0, & \text{otherwise} \end{cases} \quad (14)$$

The corresponding Fourier excitation for the sub-sectioned time sequence can be given as [13]:

$$a_{mn} = \frac{(t_2 - t_1)}{T_p} [\sin c\{m\pi f_p(t_2 - t_1)\}] e^{-jm\pi f_p(2t_1 + \tau_{n1})} + \frac{(t_4 - t_3)}{T_p} [\sin c\{m\pi f_p(t_4 - t_3)\}] e^{-jm\pi f_p(2t_3 + \tau_{n2})} \quad (15)$$

The complex excitation coefficient for the time scheme shown in Fig. 2(c) can be simplified as:

$$a_{mn} = \xi_{n1} \{\sin c(m\pi \xi_{n1})\} e^{-jm\pi(2\delta_{n1} + \xi_{n1})} + \xi_{n2} \{\sin c(m\pi \xi_{n2})\} e^{-jm\pi(2\delta_{n2} + \xi_{n2})} \quad (16)$$

where  $\xi_{n1}$  and  $\xi_{n2}$  are the normalized on-time durations of the sub-pulses shown in Fig. 2(c). The normalized starting instants of the sub-pulses are denoted as  $\delta_{n1} (= t_1/T_p)$  and  $\delta_{n2} (= t_3/T_p)$ . It is clear from equations (10), (13), and (16) that an additional degree of freedom in terms of  $\delta_n$  is available for modified time schemes compared to simple on-off time scheme. This additional freedom can be suitably explored to control the harmonic radiations without affecting the fundamental pattern.

**Problem formulation**

The objectives of simultaneous suppression of SLL and SBLs, as well as directivity enhancement of 16-element TMLA, is addressed in this paper by proposing a unique outer-element controlled time sequence along with optimized excitations ( $I_n$ ). The normalized starting instants ( $\delta_n$ ) and the on-time periods ( $\xi_n$ ) of only four outer elements are optimized to get the proposed time sequence. The SLL and all the undesired harmonic radiation patterns (SBLs) are minimized with a constraint on beamwidth to achieve a high-directive radiation pattern.

Other SBL reduction methods using shifted and sub-sectioned optimized time sequences are also presented, and the outcomes of these methods are compared with the proposed method. For an optimally shifted time sequence, the normalized switch-on instants ( $\delta_n$ ) of each array element are optimized along with the duration of on-states ( $\xi_n$ ) by considering uniform excitations ( $I_n = 1$ ). Another method of SBL reduction is also demonstrated with a sub-sectioned optimal time scheme, where the switching instants ( $\delta_{n1}, \delta_{n2}$ ) and the normalized on-times ( $\xi_{n1}, \xi_{n2}$ ) of the sub-pulses are simultaneously optimized by keeping the static excitations uniform ( $I_n = 1$ ). For all these methods, the uniform spacing between the radiating elements is also optimized.

The cost function (CF) for the minimization problem is designed as:

$$CF = w_1 \times (SLL_0^{(i)})|_{f_0} + w_2 \times (SBL_m^{(i)})|_{f_0 + mf_p} + w_3 \times FNBW^{(i)} \quad (17)$$

where  $SLL_0$  and  $SBL_m$  are the maximum level of sidelobe for the fundamental pattern at  $f_0$  and the maximum level of sidebands for the harmonic patterns at  $f_0 + mf_p$  ( $m = \pm 1, \pm 2, \dots, \pm \infty$ ),  $FNBW$  denotes the beamwidth between the first nulls, and  $w_1, w_2, w_3$  represent the contributing weights. The contributing factors are equally weighted ( $w_1 = w_2 = w_3 = 1$ ) for the simultaneous suppression of SLL and SBLs. The target is to lower the maximum SLL of the fundamental pattern below  $-40$  dB and all the higher sidebands as low as possible at the same time. For higher order SBLs, first 20 harmonic patterns ( $|m| = 20$ ) are considered in the optimization process. The power dispersed in higher order sidebands are also calculated to show the decaying nature of SBLs.

Different cases of SLL and SBL reduction approaches are explored by using the modified versions of PSO. The optimal solutions are achieved by employing a NPSOWM. The numerical results obtained from traditional PSO and NPSO-based strategies for different SLL and SBL reduction methods are also presented to show the performance superiority of the NPSOWM-based approach. PSO is a familiar swarm intelligence-based computational technique used to solve diverse electromagnetic problems [43]. To enhance the global search ability of traditional PSO, a modified version of PSO termed as novel PSO has been proposed [44]. Further modifications have been made to PSO for fine-tuning of a solution by introducing a wavelet theory-based mutation process [45]. The wavelet mutation (WM) differs from the conventional mutation of PSO by incorporating a balance between the exploration and exploitation of the search space. A broader search space at the initial stages of optimization process for the better exploration, and a relatively narrower search space at the final stages for the fine-tuning of the desired solution can be attained by NPSOWM. In this way, a global optimum solution for the above-mentioned optimization problem is achieved by outperforming the solutions from NPSO and PSO. A detailed

**Table 1.** Control parameter values of different optimization strategies

Control parameters	PSO	NPSO	NPSOWM
Number of particles ( $n_p$ )	100	100	100
Iteration cycles ( $i$ )	300	300	300
Inertia weight ( $w$ )	0.5	-	-
Shape parameter ( $\xi_{wm}$ )	-	-	2.5
Mutation probability ( $p_m$ )	-	-	0.05
Upper limit of dilation parameter ( $g$ )	-	-	10 000
Acceleration coefficients ( $C_1, C_2$ )	1.5	1.5	1.5

discussion of NPSOWM, NPSO, and PSO can be found in [46]. For the SLL and SBL reduction problems discussed in this work, the search ranges of the modeling parameters are predefined. The search ranges for the normalized on-time duration ( $\xi_n$ ), switch-on instants ( $\delta_n$ ), and inter-element spacing ( $d$ ) are considered as  $[0.01, 1]$ ,  $[0.1, 1]$ , and  $[0.5\lambda_0, \lambda_0]$ . The best-proven values of control parameters for the applied optimization strategies, obtained after several runs, are presented in Table 1.

### Numerical assessment

Three different cases of SLL and SBL reduction methods are discussed in this section. The first two cases of SLL and SBL reduction with optimally shifted and sub-sectioned pulses are presented for an exhaustive comparison of different approaches with the employed optimization algorithms. Shifted pulses within the modulation period generally considered beneficial for the SBL reduction. Dividing the total on-time periods into multiple subsections further decreases the SBLs. The proposed method demonstrated in the third case has extended this idea by incorporating an outer-element controlled optimized time sequence for SLL and SBL reduction. The results obtained by this method is also assessed for all the employed optimization techniques, and also compared with other two methods to show the superiority of the proposed method. The first case is concerned with an optimally shifted time scheme where the starting instants of each element and the total on-time periods are optimized. The spacing between elements is also considered for optimization by keeping the amplitude excitations uniform. The second case is devoted to a sub-sectioned time scheme with uniform excitation where the starting instants and on-time durations of each sub-pulses are simultaneously optimized along with the uniform element spacing of the array. The discussion of the outer-element controlled time scheme in the third case is considered as the proposed method to get the desired solutions. In this case, an optimal time sequence, along with optimized excitation coefficients, is developed to suppress the SLL and SBLs simultaneously. The results obtained from the first two cases are compared with this case to show the performance superiority of the proposed method. For all three cases, PSO- and NPSO-based results are presented along with the optimal solutions obtained from NPSOWM.

The proposed method is also compared with a  $-30$  dB reference Chebyshev pattern to show the improvements in terms of SLLs and SBLs. The time sequence of a  $-30$  dB Chebyshev pattern for the 16-element TMLA is shown in Fig. 3. The normalized power patterns for the fundamental ( $m=0$ ), first positive ( $m=1$ ), and second positive ( $m=2$ ) sidebands are presented in

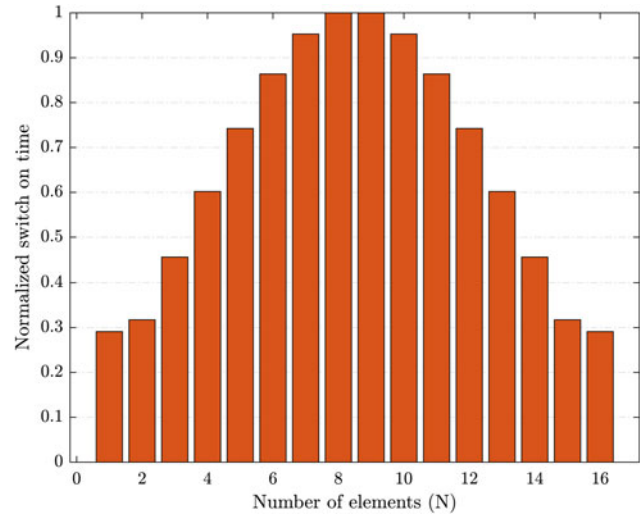
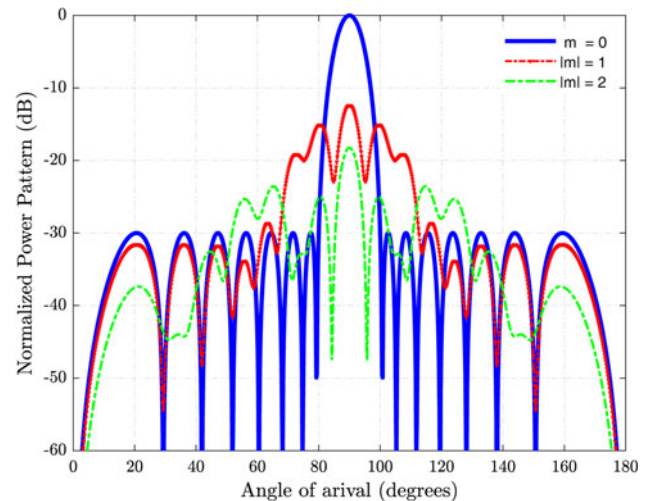
**Fig. 3.** Normalized on-time sequence of a  $-30$  dB Chebyshev pattern for 16-element TMLA.**Fig. 4.** Normalized radiation patterns of the fundamental and first two positive sidebands using a  $-30$  dB Chebyshev time scheme.

Fig. 4. The array is uniformly spaced with  $0.5\lambda_0$ , and operating at 3 GHz ( $f_0$ ) along with a modulating frequency of 1 MHz ( $f_p$ ). The first two SBLs of the reference Chebyshev pattern is obtained as  $SBL_1 = -12.39$  dB and  $SBL_2 = -18.25$  dB. The directivity is calculated as 10.8819 dB. The radiation properties of a uniform 16-element TMLA is also calculated using MATLAB. The SLL, half-power beamwidth (HPBW), FNBW, and directivity of uniform TMLA are  $-13.15$  dB,  $6.48^\circ$ ,  $14.4^\circ$ , and 12.04 dB.

### Case 1: time scheme with optimally shifted pulses and uniform excitations

The first approach of suppressing SLL and SBLs is concerned with an optimal pulse-shifted time scheme, where the normalized starting instants ( $\delta_n$ ) of radiating elements, as well as the duration of on-times ( $\xi_n$ ), are optimized within the specified search ranges. The number of variables used in the optimization are the starting instants of 10 elements ( $\delta_1, \delta_2, \dots, \delta_5$  and  $\delta_{12}, \delta_{13}, \dots, \delta_{16}$ ). The on-time duration of each element ( $\xi_1, \xi_2, \xi_3, \dots, \xi_{16}$ ) along

**Table 2.** Numerical results obtained with different optimization algorithms for case 1

Algorithms	SLL (dB)	SBL <sub>1</sub> (dB)	SBL <sub>2</sub> (dB)	HPBW (°)	FNBW (°)	P <sub>0</sub> (%)	P <sub>SB</sub> (%)	Directivity (dB)
PSO	-26.94	-18.30	-22.00	5.76	14.76	64.04	35.95	12.3776
NPSO	-27.59	-18.25	-21.22	5.76	14.76	59.65	40.34	12.2325
NPSOWM	-31.04	-18.15	-21.02	5.76	14.76	60.04	39.95	12.2127

with the uniform spacing ( $d$ ) between them ( $d_1 = d_2 = d_3 = \dots = d_{16} = d$ ) are also optimized. Thus, a total number of 27 variables are considered for optimization against the selected total number of particles of 100. The ratio between the number of particles to the total number of variables are calculated as 3.70 : 1 for all the applied optimization algorithms. The excitations are considered uniform ( $I_n = 1$ ), and the optimization processes are performed with PSO, NPSO, and NPSOWM. The uniform element spacings of the array for PSO-, NPSO-, and NPSOWM-based approaches are optimized as  $0.8169\lambda_0$ ,  $0.7892\lambda_0$ , and  $0.8692\lambda_0$ . The reduced SLLs obtained with PSO, NPSO, and NPSOWM are -26.94, -27.59, and -31.04 dB, respectively. The SBLs are suppressed simultaneously, and the values of SBL<sub>1</sub> and SBL<sub>2</sub> obtained with PSO, NPSO, and NPSOWM are -18.30, -18.25, -18.15, and -22, -21.22, -21.02 dB, respectively. The directivities of the 16-element TMLA optimized with PSO, NPSO, and NPSOWM are reported as 12.3776, 12.2325, and 12.2127 dB. All the numerical outcomes obtained with the employed optimization techniques are presented in Table 2 for a fair comparison. It is evident from Table 2 that the NPSOWM-based result is better than PSO and NPSO-based results in terms of SLLs. The NPSOWM technique also improves the SLL with -31.04 dB contrasted to -13.15 and -30 dB of the uniform and Chebyshev patterns, respectively. The SBLs of -12.39 and -18.25 dB of the reference Chebyshev pattern is also reduced to -18.15 and -21.02 dB with NPSOWM. The directivities are also enhanced to 12.2127 dB from 10.8819 and 12.04 dB of the Chebyshev and uniform patterns.

The optimal on-time sequence derived with NPSOWM is presented in Fig. 5. The corresponding optimal power patterns for the fundamental ( $m=0$ ) and first two sidebands ( $m=1, 2$ ) are shown in Fig. 6. The higher-order sidebands ( $m > 2$ ) are also reduced, and the first 20 positive SBLs obtained with different optimization techniques are presented in Fig. 7. All the SBLs are reduced below the level of the first two SBLs, which implies that simultaneous reduction of SLLs and SBLs is achieved. The radiated power by fundamental and first 10 sideband patterns obtained with all three optimization processes is shown in Fig. 8. The power in fundamental patterns is reported as 64.04, 59.65, and 60.04% with PSO, NPSO, and NPSOWM-based strategies. The radiated power in the first and second sidebands is also suppressed below 12 and 5% of the total power radiated with all three optimization techniques. The wasted power in all the sidebands is reported as 35.95, 40.34, and 39.95% obtained with PSO, NPSO, and NPSOWM.

**Case 2: time scheme with optimal sub-sectioned pulses and uniform excitations**

The second approach of SLL and SBL reduction is discussed in this section by an optimally derived sub-sectioned time scheme, where the normalized on-time durations ( $\xi_{n1}$ ,  $\xi_{n2}$ ) and the

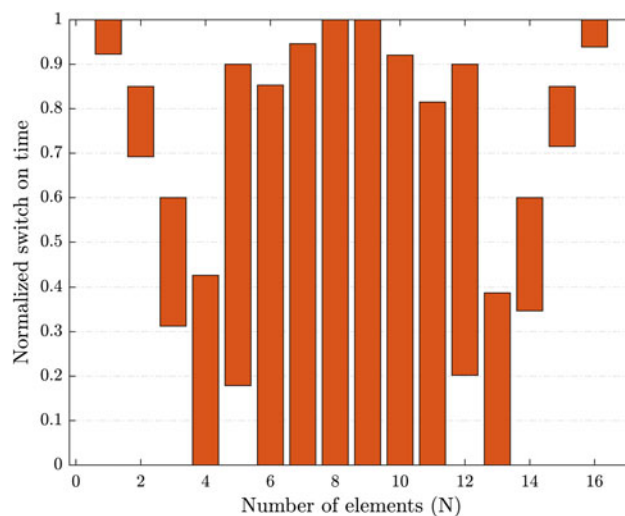


**Fig. 5.** Normalized on-time sequence obtained by NPSOWM for 16-element TMLA (case 1).

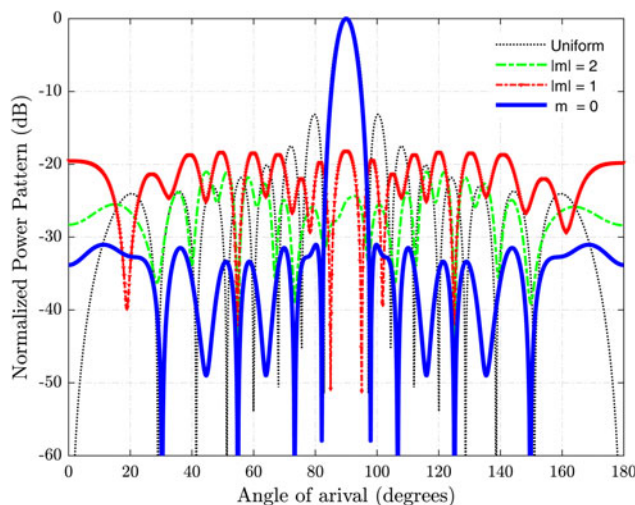


**Fig. 6.** Normalized radiation patterns of the fundamental and first two sidebands obtained by NPSOWM (case 1).

normalized on-time instants ( $\delta_{n1}$ ,  $\delta_{n2}$ ) of the sub-pulses are optimized within the specified search ranges. The number of variables considered in this case are the on-time instants of the second pulse ( $n=2$ ) for 14 elements ( $\delta_{n1}$ ,  $\delta_{n2}$ , ...,  $\delta_{n7}$  and  $\delta_{n10}$ ,  $\delta_{n11}$ , ...,  $\delta_{n16}$ ) where the starting instants of the first pulse ( $n=1$ ) for all the elements are considered 0 (as all the elements are switched on at the starting). The sub-sectioned (in two parts) on-time duration of each element except for the central two elements i.e. 28 number of variables and the uniform spacing

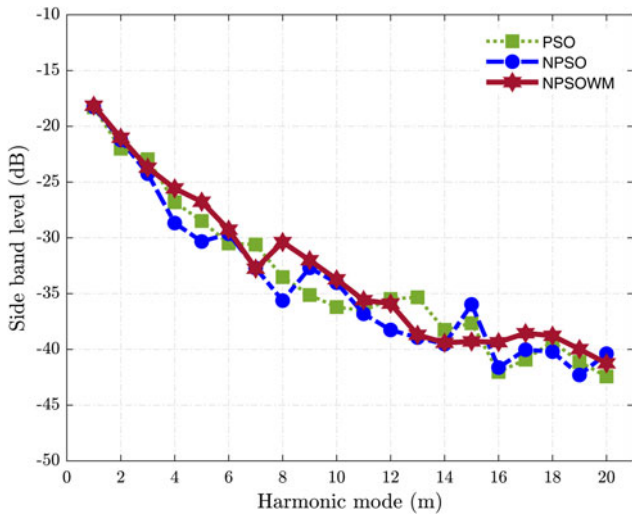


Fig. 7. First twenty SBLs for 16-element TMLA obtained by different optimization strategies (case 1).

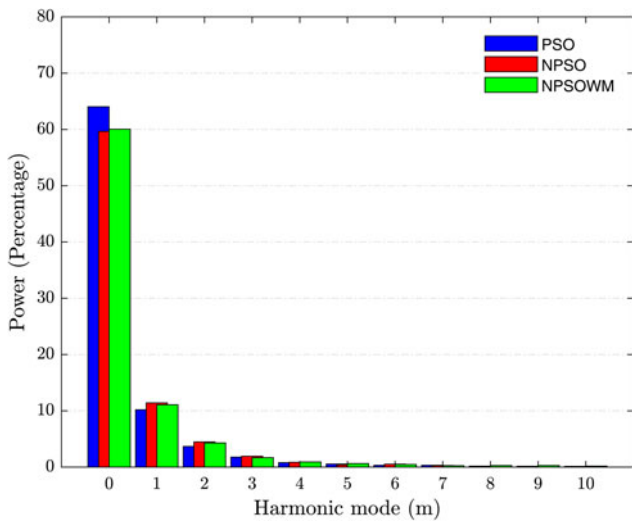


Fig. 8. Radiated power in the fundamental and first ten positive sidebands obtained by different optimization strategies (case 1).

( $d$ ) between them are also optimized. Thus, a total number of 43 variables are considered for optimization. The swarm size or the total number of particles for PSO, NPSO, and NPSOWM are 100. So, the ratio between the number of particles to the total number of variables are calculated as 2.32 : 1 for all the optimization algorithms. The excitations are considered uniform ( $I_n = 1$ ), and the optimized inter-element spacings are obtained as  $0.7442\lambda_0$ ,  $0.7607\lambda_0$ , and  $0.8012\lambda_0$  with PSO, NPSO, and

NPSOWM. The SLL,  $SBL_1$ ,  $SBL_2$ , and directivity attained with NPSOWM are  $-34.57$ ,  $-22.18$ ,  $-19.23$ , and  $12.6857$  dB, respectively. The SLLs of  $-30.67$  and  $-31.89$  dB are obtained with PSO and NPSO. The values of  $SBL_1$  and  $SBL_2$  are reported as  $-21.59$ ,  $-20.36$ , and  $-21.79$ ,  $-19.95$  dB with PSO and NPSO-based strategies, respectively. The directivities obtained by PSO and NPSO are  $12.6046$  and  $12.6258$  dB, respectively. The numerical results attained with all three employed optimization techniques are presented in Table 3. The NPSOWM-based approach shows better results in terms of SLL and  $SBL_1$ . The optimal results achieved by all three optimization strategies outperform the results obtained with the reference Chebyshev pattern.

The optimal sub-sectioned time scheme obtained by NPSOWM is presented in Fig. 9. The optimal radiation patterns achieved by NPSOWM-based time scheme for the fundamental pattern ( $m = 0$ ) and the first two sidebands ( $m = 1, 2$ ) are presented in Fig. 10. The higher-order sidebands ( $m > 2$ ) up to the first 20 positive SBLs for different versions of PSO are shown in Fig. 11. The power in the fundamental pattern and first 10 positive sidebands obtained by PSO, NPSO, and NPSOWM are presented in Fig. 12. The radiated power in fundamental patterns is reported as 66.83, 66.05, and 64.27% with PSO, NPSO, and NPSOWM, respectively. The power radiated by individual sidebands is reduced below 6% with all three optimization strategies. The wasted power in undesired sidebands is calculated as 33.16, 33.94, and 35.72% obtained with PSO, NPSO, and NPSOWM.

Case 3: outer-element controlled time scheme and optimized excitations

This section is devoted to analyzing and assessing the proposed SLL and SBL reduction method with optimally controlled outer elements and optimized nonuniform excitations ( $I_n \neq 1$ ). Toward this purpose, the normalized starting instants ( $\delta_n$ ) and on-time durations ( $\xi_n$ ) of four edge elements of the array (element nos. 1, 2, 15, and 16) are optimized along with the uniform element spacing. For the remaining radiating elements, uniform duration of on-times ( $\xi_n = 1$ ) are considered, which also implies that element nos. 3–14 is switched on for the entire modulation period. The variables considered for optimization are the excitations of 16 elements ( $(I_1, I_2, I_3, \dots, I_{16})$ ), the total on-time duration and on-time instants of outer elements ( $\delta_1, \delta_2, \delta_{15}, \delta_{16}$  and  $\xi_1, \xi_2, \xi_{15}, \xi_{16}$ ) along with the uniform spacing ( $d$ ). Thus, a total number of 25 variables are used in the optimization process and the swarm size or the total number of particles are selected as 100. So, the ratio between the number of particles to the number of variables is calculated as 4 : 1 for the proposed case. This also implies that a better solution is obtained with the proposed method by reducing the computational burden as a smaller number of variables need to be optimized compared to the other two methods. The optimized element spacings obtained by PSO, NPSO, and NPSOWM are  $0.8416\lambda_0$ ,

Table 3. Numerical results obtained with different optimization algorithms for case 2

Algorithms	SLL (dB)	$SBL_1$ (dB)	$SBL_2$ (dB)	HPBW ( $^\circ$ )	FNBW ( $^\circ$ )	$P_0$ (%)	$P_{SB}$ (%)	Directivity (dB)
PSO	-30.67	-21.59	-20.36	5.40	14.76	66.83	33.16	12.6046
NPSO	-31.89	-21.79	-19.95	5.40	14.76	66.05	33.94	12.6258
NPSOWM	-34.57	-22.18	-19.23	5.40	14.76	64.27	35.72	12.6857

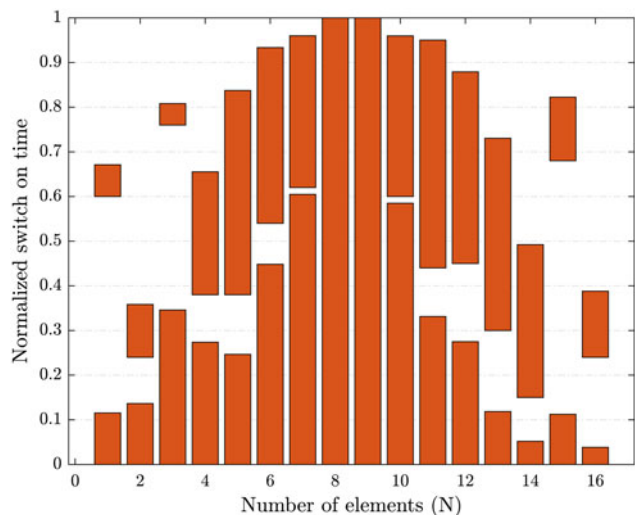


Fig. 9. Normalized on-time sequence obtained by NPSOWM for 16-element TMLA (case 2).

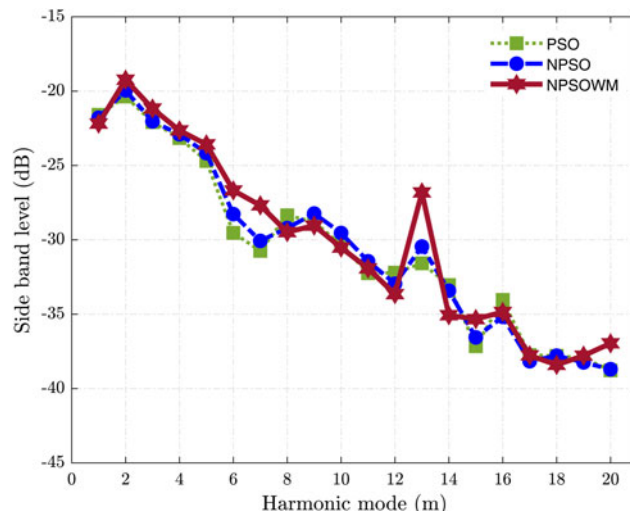


Fig. 11. First twenty SBLs for 16-element TMLA obtained by different optimization strategies (case 2).

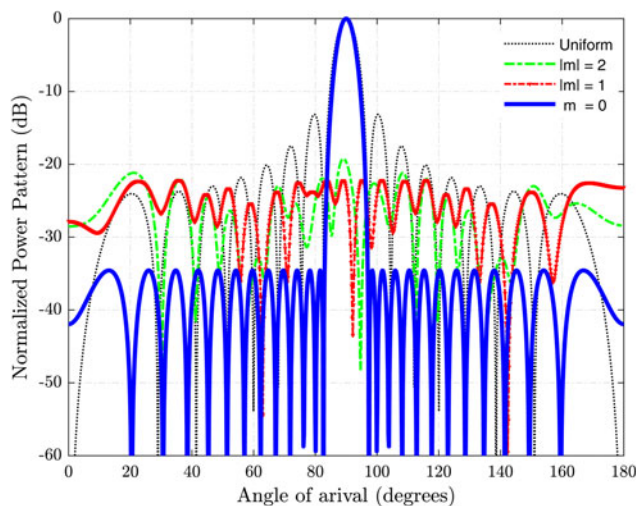


Fig. 10. Normalized radiation patterns of the fundamental and first two sidebands obtained by NPSOWM (case 2).

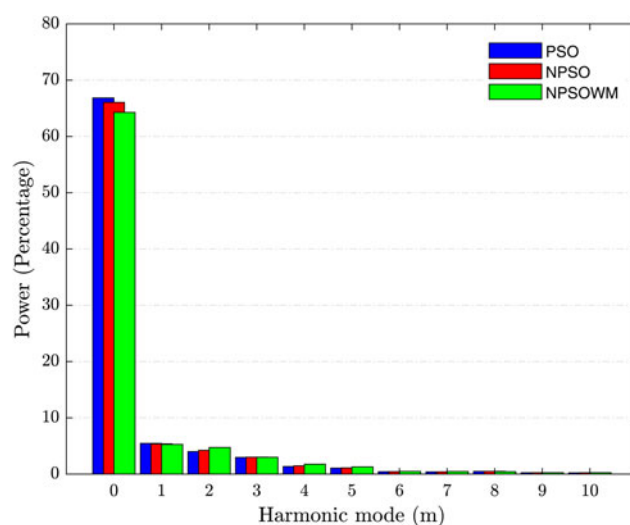


Fig. 12. Radiated power in the fundamental and first ten positive sidebands obtained by different optimization strategies (case 2).

0.8507 $\lambda_0$ , and 0.8812 $\lambda_0$ . The SLLs obtained with PSO, NPSO, and NPSOWM-based strategies are  $-38.98$ ,  $-40.90$ , and  $-43.29$  dB. The SBL<sub>1</sub> is reduced to  $-29.13$ ,  $-29.96$ , and  $-30.97$  dB with PSO, NPSO, and NPSOWM. The values of SBL<sub>2</sub> obtained with PSO, NPSO, and NPSOWM-based approaches are  $-33.06$ ,  $-33.45$ , and  $-34.13$  dB, respectively. The directivities of the array are also enhanced to 13.0584, 13.0592, and 13.1439 dB with all three optimization techniques. The results achieved with case 3 improve the SLLs and SBLs compared to the corresponding reference Chebyshev pattern and uniform pattern. The numerical results are reported in Table 4, which shows that the NPSOWM-based approach outperforms other results. The simultaneously reduced values of SLLs and SBLs obtained in case 3 also shows superior performance than the other two cases (cases 1 and 2) discussed earlier in this work.

The optimized excitations and the proposed optimal time scheme derived by NPSOWM are shown in Figs 13 and 14. The corresponding optimal power patterns at the fundamental

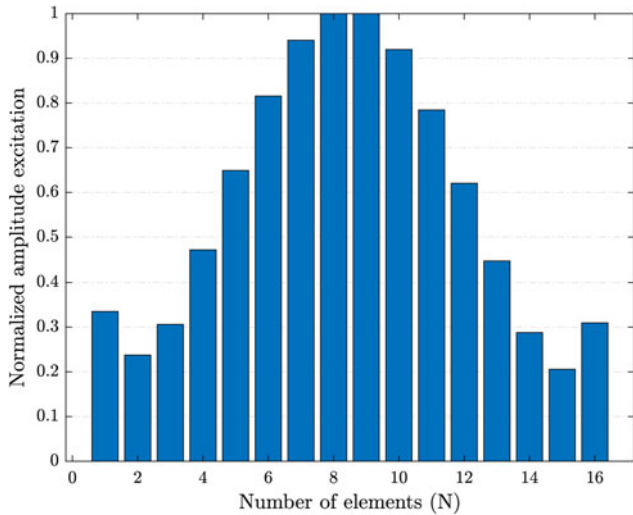
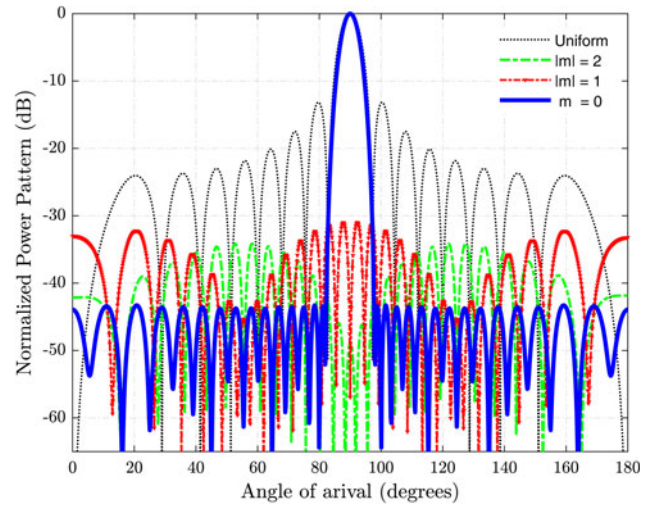
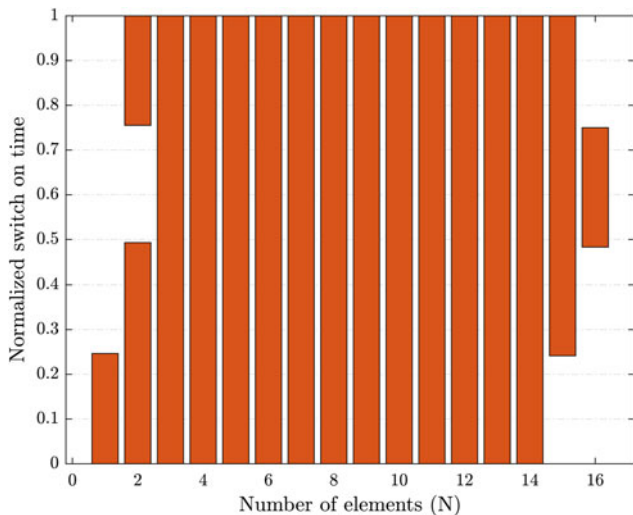
( $m = 0$ ) and first two sidebands ( $m = 1, 2$ ) obtained with the proposed method are presented in Fig. 15. The higher-order sidebands ( $m > 2$ ) are also suppressed with the proposed method, and the nature of the first twenty SBLs obtained with PSO, NPSO, and NPSOWM are shown in Fig. 16. The radiated power in optimally derived patterns up to the first ten harmonics is presented in Fig. 17. The power radiated by the desired fundamental patterns is obtained as 91.75, 93.07, and 94.37% with PSO, NPSO, and NPSOWM-based approaches. The total amount of wasted power in sidebands are reduced to 8.24, 6.92, and 5.62% with PSO, NPSO, and NPSOWM.

The optimal time sequences with periodic on-off states are beneficial for SLL and SBL reduction. But it also comes with an inherent limitation of gain reduction as the off-states in a time sequence accounts for energy absorption by high-speed switches in the feed network. The reductions in gain for case 1 due to PSO, NPSO, and NPSOWM-based time schemes are 3.3920, 3.4874, and 3.7980 dB. The gain reductions in case 2 due to



**Table 4.** Numerical results obtained with different optimization algorithms for case 3

Algorithms	SLL (dB)	SBL <sub>1</sub> (dB)	SBL <sub>2</sub> (dB)	HPBW (°)	FNBW (°)	P <sub>0</sub> (%)	P <sub>SB</sub> (%)	Directivity (dB)
PSO	-38.98	-29.13	-33.06	5.40	16.20	91.75	8.24	13.0584
NPSO	-40.90	-29.96	-33.45	5.40	16.20	93.07	6.92	13.0592
NPSOWM	-43.29	-30.97	-34.13	5.40	16.20	94.37	5.62	13.1439

**Fig. 13.** Normalized excitation amplitudes for 16-element TMLA obtained by NPSOWM (case 3).**Fig. 15.** Normalized radiation patterns of the fundamental and first two sidebands obtained by NPSOWM (case 3).**Fig. 14.** Normalized outer-element controlled time sequence obtained by NPSOWM for 16-element TMLA (case 3).

PSO, NPSO, and NPSOWM-based time schemes are reported as 3.1109, 3.2094, and 3.4047 dB. The outer element-controlled proposed time schemes have shown considerable improvements in terms of gain reduction compared to the other two cases. The reductions in gain for case 3 due to PSO, NPSO, and NPSOWM-based time sequences are achieved as 0.2353, 0.1948, and 0.1567 dB. Comparisons of different cases in terms of gain reduction are presented in Fig. 18. The NPSOWM-based result

for case 3 outperforms all other results with a minimal reduction in gain. The power handling capability is also enhanced to a great extent, with 94.37% power radiated in the desired pattern. The power in undesired sidebands is also reduced below a minimum level of 5.62%, which implies that the most efficient solution is achieved with this method compared to all other approaches discussed in this paper. The DRRs calculated for case 3 with PSO, NPSO, and NPSOWM are 4.40, 4.34, and 4.21, respectively. The DRRs obtained with other two cases can be considered 1 because of the uniform amplitude distribution. The NPSOWM-based approach with case 3 is considered as the proposed method to achieve the desired objectives and also compared with other published works to show the potency of the method. The comparisons with other published results are presented in Table 5. The convergence profiles for all the cases are shown in Figs 19–21, respectively.

The reduction in SLL observed with the proposed technique has shown a substantial improvement with -43.29 dB over -30 dB of the best-published literature results reported in [12, 13, 21, 23]. The SBL<sub>1</sub> is suppressed to -30.97 dB in comparison with -18 dB [29], -19.50 dB [12], -20 dB [21], -21 dB [29], -24.60 dB [10], -25.53 dB [23], and -27.80 dB [13] of already reported results. The SBL<sub>2</sub> is also minimized to -34.13 dB compared to -21.70 dB [12] and -25.01 dB [23] of the reported literature works. The power handling capability is also enhanced with 94.37% power radiated in the desired pattern compared to 77.58% [23], 78% [13], and 78.20% [12] reported in published literature works. The power radiated in unintended sidebands is also suppressed, and the directivity of the array is simultaneously improved with the proposed method.

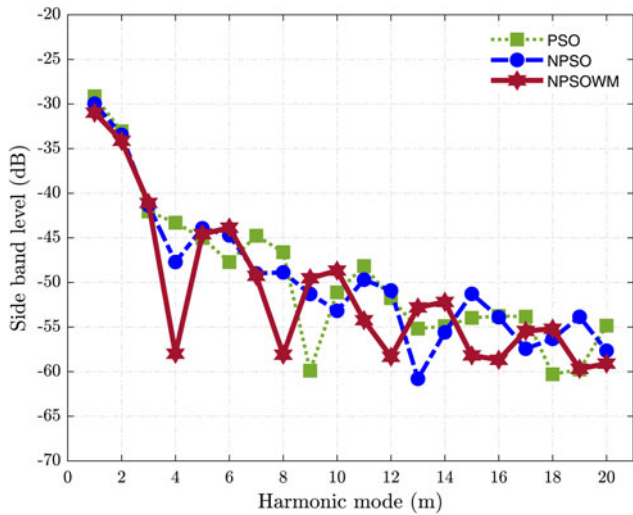


Fig. 16. First twenty SBLs for 16-element TMLA obtained by different optimization strategies (case 3).

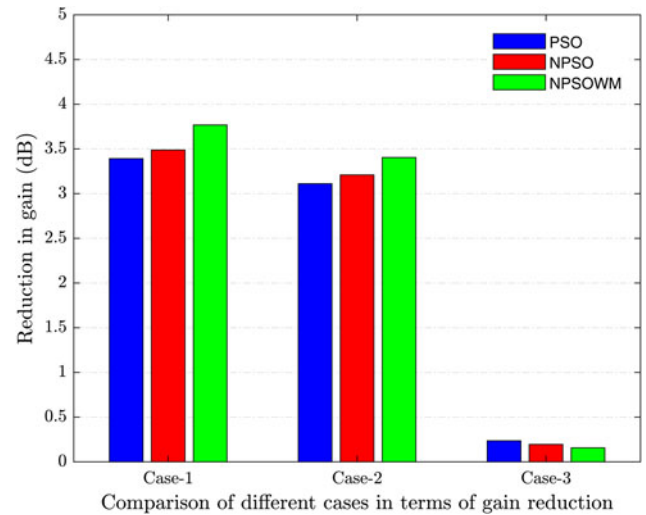


Fig. 18. Comparisons of gain reduction in case1, case 2, and case 3 due to optimized time sequences.

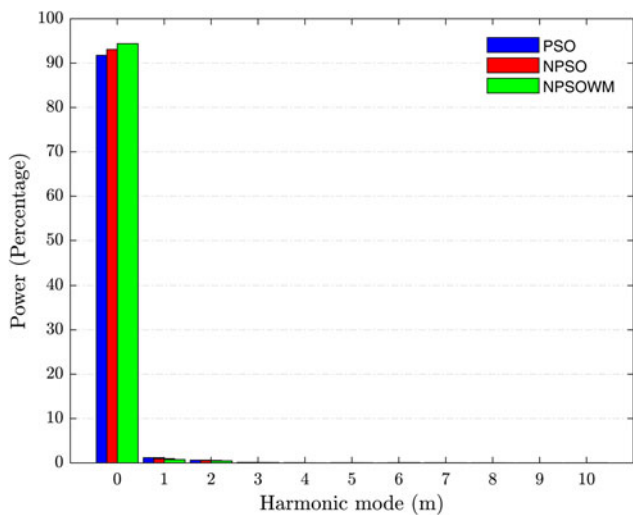


Fig. 17. Radiated power in the fundamental and first ten positive sidebands obtained by different optimization strategies (case 3).

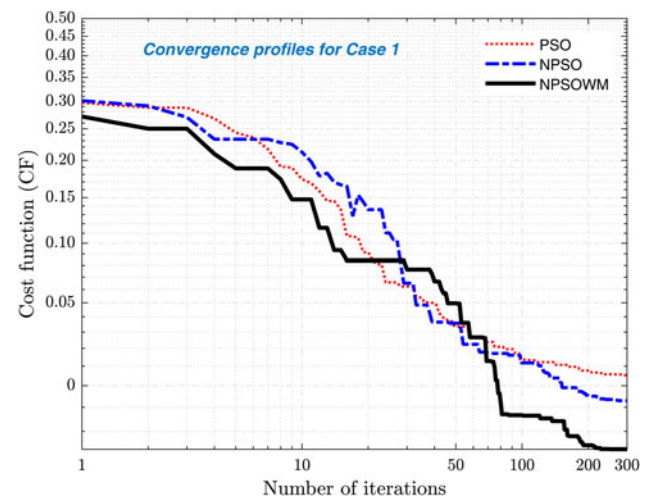


Fig. 19. Convergence profiles of all the employed optimization algorithms for case 1.

Table 5. Comparative analysis of the proposed method with other published literature works for SLL and SBL reduction

Reference papers	SLL (dB)	SBL <sub>1</sub> (dB)	SBL <sub>2</sub> (dB)	P <sub>0</sub> (%)	P <sub>SB</sub> (%)	Directivity (dB)
[10]	-25.50	-24.60	NR	NR	NR	NR
[12]	-30.00	-19.50	-21.70	78.20	21.80	NR
[13]	-30.00	-27.80	NR	78.00	22.00	10.20
[21]	-30.00	-20.00	NR	NR	NR	10.10
[23]	-30.00	-25.53	-25.01	77.58	22.42	NR
[29] Example 1	-19.00	-18.00	NR	NR	NR	NR
[29] Example 2	-20.00	-21.00	NR	NR	NR	NR
This work (proposed)	-43.29	-30.97	-34.13	94.37	5.62	13.1439

NR, not reported.

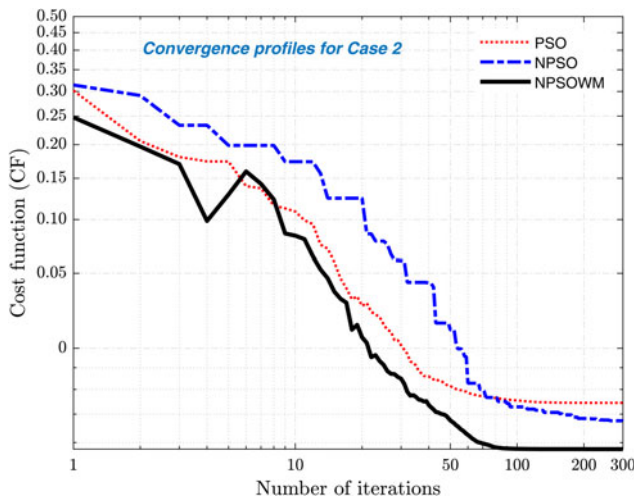


Fig. 20. Convergence profiles of all the employed optimization algorithms for case 2.

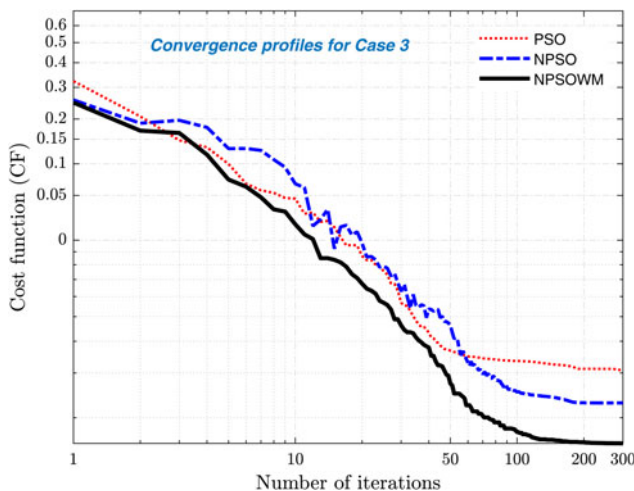


Fig. 21. Convergence profiles of all the employed optimization algorithms for case 3.

## Conclusion

An efficient design method for the simultaneous suppression of sidelobe and SRs in a TMLA is introduced in this paper. A unique outer-element controlled optimal time scheme along with optimized excitations is generated for this purpose. The proposed time scheme is derived by suitably exploiting the on-time instants and on-time durations of outer elements of the 16-element TMLA. Other sidelobe and sideband reduction methods with optimally shifted and sub-sectioned time sequences are also presented for comparative analysis. Furthermore, the obtained numerical results are assessed with a  $-30$  dB Chebyshev pattern to show the efficacies of this approach. Multiple objectives with controlled radiation features are addressed by using modified versions of the PSO algorithm. In this regard, an NPSOWM algorithm is utilized to get the optimal solutions. The optimal NPSOWM-based results are also compared with NPSO and conventional PSO-based results to show its performance superiority over the others. The numerical assessment shows that a

much-improved performance is achieved with the proposed method by reducing the SLL and SBLs to  $-43.29$ ,  $-30.97$ , and  $-34.13$  dB compared to  $-30$ ,  $-27.8$ , and  $-25.01$  dB of the already reported works. Thus, a considerable improvement of 44.3, 11.4, and 36.46% in terms of SLL,  $SBL_1$ , and  $SBL_2$  is achieved. The directivity of the TMLA is also enhanced by 28.86% from the best-published result. As compared to the reference Chebyshev pattern, the proposed TMLA has reduced the SLL and SBLs by 13.29, 18.58, and 15.88 dB. The power handling capability of the TMLA is increased to 94.37%, implying an enhanced performance by 16.17% from the best-published work. The SRs due to higher-order harmonics are suppressed, and the power wasted in sidebands is also reduced to a marginal level. Moreover, the computational load of the optimization procedure is also mitigated as only the outer four elements are optimized for the desired time scheme. Thus, an efficient solution with multiple desired objectives is achieved in a 16-element TMLA with the proposed approach.

**Acknowledgements.** This research work is part of a project funded by Science and Engineering Research Board (SERB), Department of Science and Technology (DST), Government of India (GoI) under the project grant no. EEQ/2017/000519, dated March 23rd, 2018.

## References

- Shanks HE and Bickmore RW (1959) Four-dimensional electromagnetic radiators. *Canadian Journal of Physics* **37**(3), 263–275. doi: <https://doi.org/10.1139/p59-031>.
- Haupt RL (2017) Antenna arrays in the time domain: an introduction to timed arrays. *IEEE Antennas and Propagation Magazine* **59**(3), 33–41. doi: <https://doi.org/10.1109/MAP.2017.2686082>.
- Rocca P, Oliveri G, Mailloux RJ and Massa A (2016) Unconventional phased array architectures and design methodologies – a review. *Proceedings of the IEEE* **104**(3), 544–560. doi: <https://doi.org/10.1109/JPROC.2015.2512389>.
- Rocca P, Yang F, Poli L and Yang S (2019) Time-modulated array antennas-theory, techniques, and applications. *Journal of Electromagnetic Waves and Applications* **33**(12), 1503–1531. doi: <https://doi.org/10.1080/09205071.2019.1627251>.
- Shanks HE (1961) A new technique for electronic scanning. *IRE Transactions on Antennas and Propagation* **9**(2), 162–166. doi: <https://doi.org/10.1109/TAP.1961.1144965>.
- Kummer WH, Villeneuve AT, Fong TS and Terrio FG (1963) Ultra-low sidelobes from time-modulated arrays. *IEEE Transactions on Antennas and Propagation* **11**(6), 633–639. doi: <https://doi.org/10.1109/TAP.1963.1138102>.
- Fondevila J, Brégains JC, Ares F and Moreno E (2004) Optimizing uniformly excited linear arrays through time modulation. *IEEE Antennas and Wireless Propagation Letters* **3**, 298–301. doi: <https://doi.org/10.1109/LAWP.2004.838833>.
- Yang S, Gan YB and Qing A (2002) Sideband suppression in time-modulated linear arrays by the differential evolution algorithm. *IEEE Antennas and Wireless Propagation Letters* **1**, 173–175. doi: <https://doi.org/10.1109/LAWP.2002.807789>.
- Brégains JC, Fondevila-Gómez J, Franceschetti G and Ares F (2008) Signal radiation and power losses of time-modulated arrays. *IEEE Transactions on Antennas and Propagation* **56**(6), 1799–1804. doi: <https://doi.org/10.1109/TAP.2008.923345>.
- Yang S, Gan YB, Qing A and Tan PK (2005) Design of a uniform amplitude time modulated linear array with optimized time sequences. *IEEE Transactions on Antennas and Propagation* **53**(7), 2337–2339. doi: <https://doi.org/10.1109/TAP.2005.850765>.
- Poli L, Rocca P, Manica L and Massa A (2010) Handling sideband radiations in time-modulated arrays through particle swarm optimization. *IEEE*

- Transactions on Antennas and Propagation* **58**(4), 1408–1411. doi: <https://doi.org/10.1109/TAP.2010.2041165>.
12. **Poli L, Rocca P, Manica L and Massa A** (2010) Pattern synthesis in time-modulated linear arrays through pulse shifting. *IET Microwaves, Antennas and Propagation* **4**(9), 1157–1164. doi: <https://doi.org/10.1049/iet-map.2009.0042>.
  13. **Zhu Q, Yang S, Zheng L and Nie Z** (2012) Design of a low sidelobe time modulated linear array with uniform amplitude and sub-sectional optimized time steps. *IEEE Transactions on Antennas and Propagation* **60** (9), 4436–4439. doi: <https://doi.org/10.1109/TAP.2012.2207082>.
  14. **Tong Y and Tennant A** (2012) Sideband level suppression in time-modulated linear arrays using modified switching sequences and fixed bandwidth elements. *Electronics Letters* **48**(1), 10–11. doi: <https://doi.org/10.1049/el.2011.2378>.
  15. **Aksoy E and Afacan E** (2010) Thinned nonuniform amplitude time-modulated linear arrays. *IEEE Antennas and Wireless Propagation Letters* **9**, 514–517. doi: <https://doi.org/10.1109/LAWP.2010.2051312>.
  16. **Yang F, Yang S, Chen Y and Qu S** (2017) A joint optimization approach for the synthesis of large 4-D heterogeneous antenna arrays. *IEEE Transactions on Antennas and Propagation* **65**(9), 4585–4594. doi: <https://doi.org/10.1109/TAP.2017.2725379>.
  17. **Yang F, Yang S, Chen Y, Qu S and Hu J** (2018) Convex optimization of pencil beams through large-scale 4-D antenna arrays. *IEEE Transactions on Antennas and Propagation* **66**(7), 3453–3462. doi: <https://doi.org/10.1109/TAP.2018.2829875>.
  18. **Yang F, Yang S, Member S, Chen Y and Member S** (2019) Efficient pencil beam synthesis in 4-D antenna arrays using an iterative convex optimization algorithm. *IEEE Transactions on Antennas and Propagation* **67** (11), 6847–6858. doi: <https://doi.org/10.1109/TAP.2019.2922817>.
  19. **Yang F, Yang S, Chen Y and Guo J** (2019) An effective hybrid approach for the synthesis of pencil beams and shaped beams through 4D linear antenna arrays with constrained DRR. *Journal of Electromagnetic Waves and Applications* **33**(5), 584–600. doi: <https://doi.org/10.1080/09205071.2018.1564704>.
  20. **Chakraborty A, Ram G and Mandal D** (2020) Optimal pulse shifting in timed antenna array for simultaneous reduction of sidelobe and sideband level. *IEEE Access* **8**, 131063–131075. doi: <https://doi.org/10.1109/ACCESS.2020.3010047>.
  21. **Zhu Q, Yang S, Yao R and Nie Z** (2012) Gain improvement in time-modulated linear arrays using SPDT switches. *IEEE Antennas and Wireless Propagation Letters* **11**, 994–997. doi: <https://doi.org/10.1109/LAWP.2012.2213292>.
  22. **Rocca P, Poli L and Massa A** (2012) Instantaneous directivity optimisation in time-modulated array receivers. *IET Microwaves, Antennas and Propagation* **6**(14), 1590–1597. doi: <https://doi.org/10.1049/iet-map.2012.0400>.
  23. **Chen J, Liang X, He C, Fan H, Zhu W, Geng J and Jin R** (2018) Instantaneous gain optimization in time modulated array using reconfigurable power divide/combiner. *IEEE Antennas and Wireless Propagation Letters* **17**(4), 530–533. doi: <https://doi.org/10.1109/LAWP.2018.2795008>.
  24. **Bekele ET, Poli L, Rocca P, D'Urso M and Massa A** (2013) Pulse-shaping strategy for time modulated arrays – analysis and design. *IEEE Transactions on Antennas and Propagation* **61**(7), 3525–3537. doi: <https://doi.org/10.1109/TAP.2013.2256096>.
  25. **Zhu Q, Yang S, Yao R, Huang M and Nie Z** (2013) Unified time-and frequency-domain study on time-modulated arrays. *IEEE Transactions on Antennas and Propagation* **61**(6), 3069–3076. doi: <https://doi.org/10.1109/TAP.2013.2253538>.
  26. **Rocca P, Masotti D, Costanzo A, Salucci M and Poli L** (2017) The role of accurate dynamic analysis for evaluating time-modulated arrays performance. *IEEE Antennas and Wireless Propagation Letters* **16**, 2663–2666. doi: <https://doi.org/10.1109/LAWP.2017.2740359>.
  27. **Masotti D, Poli L, Salucci M, Rocca P and Costanzo A** (2019) An effective procedure for nonlinear dynamic optimization of time-modulated arrays. *IEEE Antennas and Wireless Propagation Letters* **18**(10), 2204–2208. doi: <https://doi.org/10.1109/LAWP.2019.2940280>.
  28. **Li G, Yang S and Nie Z** (2010) Direction of arrival estimation in time modulated linear arrays with unidirectional phase center motion. *IEEE Transactions on Antennas and Propagation* **58**(4), 1105–1111. doi: <https://doi.org/10.1109/TAP.2010.2041313>.
  29. **Guo J, Yang S, Qu SW, Hu J and Nie Z** (2015) A study on linear frequency modulation signal transmission by 4-D antenna arrays. *IEEE Transactions on Antennas and Propagation* **63**(12), 5409–5416. doi: <https://doi.org/10.1109/TAP.2015.2493559>.
  30. **Maneiro-Catoira R, Brégains J, García-Naya JA and Castedo L** (2017) Time modulated arrays: from their origin to their utilization in wireless communication systems. *Sensors (Switzerland)* **17**(3), 1–14. doi: <https://doi.org/10.3390/s17030590>.
  31. **Poli L, Rocca P, Oliveri G and Massa A** (2011) Harmonic beamforming in time-modulated linear arrays. *IEEE Transactions on Antennas and Propagation* **59**(7), 2538–2545. doi: <https://doi.org/10.1109/TAP.2011.2152323>.
  32. **Li H, Chen Y and Yang S** (2019) Harmonic beamforming in antenna array with time-modulated amplitude-phase weighting technique. *IEEE Transactions on Antennas and Propagation* **67**(10), 6461–6472. doi: <https://doi.org/10.1109/TAP.2019.2922815>.
  33. **Gassab O, Azrar A, Dahimene A, Bouguerra S and He C** (2020) Efficient electronic beam steering method in time modulated linear arrays. *IET Microwaves, Antennas and Propagation* **14**(5), 402–408. doi: <https://doi.org/10.1049/iet-map.2019.0673>.
  34. **Chakraborty A, Mandal D and Ram G** (2019) Beam steering in a time switched antenna array with reduced side lobe level using evolutionary optimization technique. *2019 IEEE Indian Conf. Antennas Propagation, InCAP 2019*. doi: <https://doi.org/10.1109/InCAP47789.2019.9134497>.
  35. **Chakraborty A, Ram G and Mandal D** (2021) Pattern synthesis of timed antenna array with the exploitation and suppression of harmonic radiation. *International Journal of Communication Systems* **34**(4), e4727. doi: <https://doi.org/10.1002/dac.4727>.
  36. **Chakraborty A, Ram G and Mandal D** (2021) Multibeam steered pattern synthesis in time-modulated antenna array with controlled harmonic radiation. *International Journal of RF and Microwave Computer-Aided Engineering* **31**(5), e22597. doi: <https://doi.org/10.1002/mmc.22597>.
  37. **Chakraborty A, Ram G and Mandal D** (2021) Time-modulated multi-beam steered antenna array synthesis with optimally designed switching sequence. *International Journal of Communication Systems* **34**(9), e4828. doi: <https://doi.org/10.1002/dac.4828>.
  38. **Poli L, Masotti D, Hannan MA, Costanzo A and Rocca P** (2020) Codesign of switching sequence and diode parameters for multiple pattern optimization in time-modulated arrays. *IEEE Antennas and Wireless Propagation Letters* **19**(11), 1852–1856. doi: <https://doi.org/10.1109/LAWP.2020.3010824>.
  39. **Rocca P, Zhu Q, Bekele ET, Yang S and Massa A** (2014) 4-D arrays as enabling technology for cognitive radio systems. *IEEE Transactions on Antennas and Propagation* **62**(3), 1102–1116. doi: <https://doi.org/10.1109/TAP.2013.2288109>.
  40. **Poli L, Rocca P, Oliveri G, Chuan M, Mazzucco C, Verzura S, Lombardi R and Massa A** (2018) Advanced pulse sequence design in time-modulated arrays for cognitive radio. *IEEE Antennas and Wireless Propagation Letters* **17**(5), 898–902. doi: <https://doi.org/10.1109/LAWP.2018.2821715>.
  41. **Bogdan G, Godziszewski K and Yashchyshyn Y** (2020) Experimental investigation of beam-steering applied to 2 × 2 MIMO system with single receiving RF chain and time-modulated antenna array. *International Journal of Microwave and Wireless Technologies* **12**(6), 504–512. doi: <https://doi.org/10.1017/S1759078720000744>.
  42. **Ni D, Yang S, Chen Y and Guo J** (2017) A study on the application of subarrayed time-modulated arrays to MIMO radar. *IEEE Antennas and Wireless Propagation Letters* **16**, 1171–1174. doi: <https://doi.org/10.1109/LAWP.2016.2626478>.
  43. **Robinson J and Rahmat-Samii Y** (2004) Particle swarm optimization in electromagnetics. *IEEE Transactions on Antennas and Propagation* **52**(2), 397–407. doi: <https://doi.org/10.1109/TAP.2004.823969>.

44. **Mandal D, Ghoshal SP and Bhattacharjee AK** (2010) Novel particle swarm optimization based synthesis of concentric circular antenna array for broadside radiation. *Lecture Notes in Computer Science (including its subseries Lecture Notes in Artificial Intelligence and Lecture Notes* **6466**, 432–439. doi: [https://doi.org/10.1007/978-3-642-17563-3\\_52](https://doi.org/10.1007/978-3-642-17563-3_52).
45. **Ling SH, Iu HHC, Leung FHF and Chan KY** (2008) Improved hybrid particle swarm optimized wavelet neural network for modeling the development of fluid dispensing for electronic packaging. *IEEE Transactions on Industrial Electronics* **55**(9), 3447–3460. doi: <https://doi.org/10.1109/TIE.2008.922599>.
46. **Ram G, Mandal D, Kar R and Ghoshal SP** (2016) Improvement in various radiation characteristics of time modulated linear antenna arrays using evolutionary algorithms. *Journal of Experimental and Theoretical Artificial Intelligence* **28**, 151–180. doi: <https://doi.org/10.1080/0952813X.2015.1020522>.



**Avishek Chakraborty** obtained his B.Tech. degree in electronics and communication engineering. He received his M.Tech. degree in radio physics and electronics with a specialization in space science and microwaves from the University of Calcutta, West Bengal, India, in 2017. He is presently working as a senior project fellow in a DST-SERB funded project at the National Institute of Technology, Durgapur,

West Bengal, India. He is also pursuing the Ph.D. degree as a full-time research scholar in the Department of Electronics and Communication Engineering, National Institute of Technology, Durgapur. His current research interests include antenna array synthesis, application of soft computing in antenna array optimization, and radar signal processing.



**Gopi Ram** obtained his B.E. degree in “electronics and telecommunication engineering,” from Government Engineering College, Jagdalpur, Chhattisgarh, India in 2007. He received his M.Tech. degree in “telecommunication engineering” from the National Institute of Technology, Durgapur, West Bengal, India in 2011. He joined as a full-time institute research scholar in 2012 at the National Institute of

Technology, Durgapur to carry out research for the Ph.D. degree. He received the scholarship from the Ministry of Human Resource and Development (MHRD), Government of India for the period 2009–2011 (M.Tech.) and 2012–2015 (Ph.D.). His research interest includes analysis and synthesis of antenna arrays via bio-inspired evolutionary algorithms and antenna array optimization of various radiation characteristics. He has published more than 50 research papers in international journals and conferences.



**Durbadal Mandal** obtained his B.E. degree in electronics and communication engineering, from Regional Engineering College, Durgapur, West Bengal, India in 1996. He received his M.Tech. and Ph.D. degrees from the National Institute of Technology, Durgapur, West Bengal, India in 2008 and 2011, respectively. Presently, he is attached with the National Institute of Technology, Durgapur, West Bengal,

India, as associate professor in the Department of Electronics and Communication Engineering. His research interest includes array antenna design and filter optimization via evolutionary computing techniques. He has published more than 350 research papers in international journals and conferences.